MICROMECHANICS OF COMPOSITES WITH INTEGRATED SHEAR THICKENING FLUIDS

R. Cristian Neagu, Christian Fischer, Pierre-Etienne Bourban,
and Jan-Anders E. Månson

Laboratoire de Technologie des Composites et Polymères (LTC)
Ecole Polytechnique Fédérale de Lausanne (EPFL), CH-1015 Lausanne, Switzerland
cristian.neagu@epfl.ch

ABSTRACT

In the current paper, a micromechanical model was used to predict the damping of a composite material containing shear thickening fluids (STFs) at the fibre-matrix interfaces. Predictions of the model and dynamic mechanical analysis results are in concert. The damping of the composites was improved significantly. The dynamic properties exhibited a strong dependence on both frequency and applied external load amplitude. Damping peaks appeared which coincided with the thickening of the STF at the matrix-rod interface. The location of the peaks depends on the onset of thickening and post-thickening rheological behaviour of the STF. This work shows that a micromechanics approach can be useful for an appropriate choice of microstructural design and properties of STFs in order to control the stiffness and damping behaviour of composites.

1. INTRODUCTION

1.1 Damping in composite materials

Damping is an important parameter for vibration control, noise reduction, fatigue endurance or impact resistance and has become increasingly important over the last few decades in a wide range of fields, including aeronautics, automotives and sport.

Fibre-reinforced composites possess damping mechanisms very different from those in conventional metals and alloys. At the micromechanical level, the energy dissipation is induced by different mechanisms such as the viscoelastic nature of the matrix, the damping at the fibre-matrix interface/interphase or the damping due to damage [1]. At the laminate level, damping is strongly dependent on the layer constituent properties as well as layer orientations, interlaminar effects, and stacking sequence [2].

Passive methods to enhance damping include surface damping treatments and constrained layer damping. Active methods involve integration of adaptive materials into composite structures to better control vibration and stiffness. Examples are laminates containing pre-deformed shape memory alloy wires, electro-rheological and/or magneto-rheological fluids which provide means of modifying damping properties via external stimuli [2]. These approaches have in common that they require an external power source to be activated. A way to avoid the need for an external power source is to use a material that changes its properties according to the loading conditions. Such behaviour is characteristic of shear-thickening fluids (STFs).

Fischer et al. [3] demonstrated that STFs can be integrated in dynamically loaded structures to tailor their damping and stiffness properties. In vibrating beam tests on model sandwich structures containing layers of STF, the vibration properties were significantly modified, due to simultaneous increase in stiffness and damping. Therefore, it would be desirable to investigate the potential of integrating STFs at the microscale of polymer composites to create new materials with a unique functionality, i.e. with load-controlled adaptive dynamic stiffness-damping properties. A possible application are alpine skis where STFs can be used to damp low frequencies at high amplitude deformation known to deteriorate the ski-snow contact.

1.2 Properties of shear thickening fluids

STFs are typically composed of a concentrated stabilized dispersion of rigid sub-micron particles in a carrier fluid and show a marked increase in viscosity beyond a critical shear rate [4, 5]. The shear-thickening effect is due to the build-up of large hydroclusters when the critical shear rate is reached, provoking the dramatic increase in the suspension's viscosity [4]. Beyond the end-point of the transition the viscosity may become approximately independent of or may decrease with increasing shear rate. Due to the reversibility of the phenomenon, the viscosity instantaneously goes back to initial values when releasing the shear stress.

STFs have very interesting dynamic properties. Lee and Wagner [4] demonstrated from stress–strain Lissajous plots that a dramatic increase in viscous dissipation occurs at the shear-thickening transition. Fischer et al. [5] showed that the pre- and post-transition viscosity of a colloidal suspensions of fused silica in polypropylene glycol subjected to oscillating shear is independent of the applied strain amplitude in frequency sweeps. Frequency sweeps corresponding to different set strain amplitudes showed a unique power-law decrease in the viscosity with frequency, both below and above the shear-thickening transition. Similar results were obtained for monodispersed silica particles in polyethylene glycol [6]. It was also shown that the critical shear strain for thickening can be estimated using the shear stress from steady state measurements and the complex viscosity over the entire investigated frequency range.

1.3 Scope and aim

In this work, a micromechanics approach is used to study the effect of a STF coating on the damping of the composite. A micromechanical model developed for unidirectional composites (UD) composites with Newtonian viscous interfaces [7] is adapted to UD composites with STF at the interface between the fibre and matrix. The novelty lies in accounting for the particular nonlinear rheological properties of the viscous interface, i.e. of the STF, which depend both on the interfacial shear strain and the vibration frequency. Furthermore, the model is validated with experiments.

2. MICROMECHANICS

A simple analytical micromechanical model is developed here. The model can be used to predict the viscoelastic properties of composites with STF coated fibres at different vibration frequencies.

The modelling approach is based on the composite cylinder assemblage (CCA) model of Hashin [8, 9], which was modified by He and Liu [7] to composites with Newtonian viscous interfaces. The model is used to estimate the average steady-state response of the composite with a viscous interface with viscosity changing depending on the interfacial shear strain and vibration frequency (i.e. STF). The analysis is constrained to UD composites under longitudinal shear deformation. The fibres (usually the stiff phase) are considered elastic, while viscoelastic properties are assumed for the matrix. The viscoelastic nature of the matrix cannot be ignored for many matrix materials e.g. elastomers, where the ratio between the storage modulus, G', and the loss modulus, G'', can be close to one.

The CCA model, schematically depicted in Figure 1a, assumes a spatial arrangement of randomly distributed composite cylinders of different cross-sections, with diameters ranging from finite to infinitesimal size. Each of the composite cylinders is made of a long inner circular fibre surrounded by an outer concentric matrix shell. The ratio of the diameter of the fibre and the matrix shell is constant and related to the fibre volume

fraction of the composite. It can be shown that all but the transverse effective properties of the CCA are those of one composite cylinder [9]. Hence, the overall response of the composite can be considered as the same as that of a composite cylinder shown in Figure 1b, consisting of a fibre surrounded by a matrix layer, with an outer radius $b = a\,(V_f)^{-1/2}$ where, a is the fibre radius and V_f the fibre volume fraction.

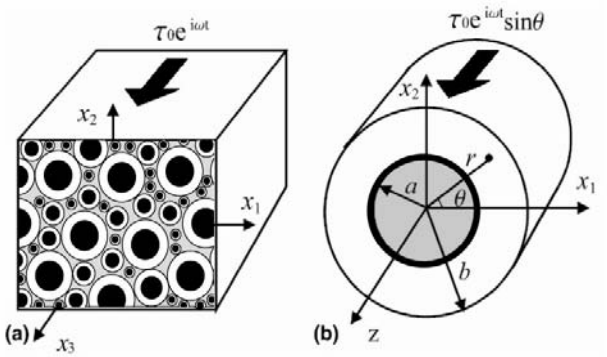

Figure 1: (a) Fibre composite subjected to a periodic longitudinal shear load, and (b) composite cylinder model with a viscous fibre-matrix interface with shear-thickening properties.

The interface between the fibre and the matrix is assumed to consist of a thin viscous STF layer with negligible thickness h. As a result, the fibre and the matrix slip with respect to each other when a shear force is applied, following the law

$$\dot{\delta}_{\mathrm{if}} = \frac{\tau^{*} h}{\eta} \tag{1}$$

where $\dot{\delta}_{\mathrm{if}}$ is the rate of sliding of the matrix relative to the fibre, i.e. the dot denoting derivative with respect on time, τ^{*} is the shear stress on the interface, and η the viscosity of the STF.

The overall mechanical response of the composite cylinder can be determined in terms of the volume averaged stress and strain. A periodic longitudinal shear load $T_3 = \tau_0 e^{i\omega t} n_2$ is applied to the composite (Figure 1a), where n_2 is the x_2 component of the outward unit normal to the surface of the composites, i is the square root of the negative unit, t is time, τ_0 and ω are the amplitude and the angular frequency of the external load, respectively. This stress state transformed to cylindrical coordinates (r,θ,z) leads to one nonzero stress component on the boundary of the composite cylinder (Figure 1b), i.e. $\tau_{rz} = \tau_0 e^{i\omega t}\sin\theta$, where θ is the angle between directions x_1 and r. Accordingly, the composite cylinder is in a state of anti-plane deformation with the displacement component, $u_z = u_z(r,\theta;t)$.

The solution for the stress and displacement field can be obtained by considering the equilibrium equations, and the fibre and matrix constitutive relations in He and Liu [7]. The boundary conditions at the fibre and matrix interface needed to solve the problem include continuity of the stress component τ_{rz}

$$\tau_{rz}^{\mathrm{m}}(r=a) = \tau_{rz}^{\mathrm{f}}(r=a) \tag{2}$$

where, superscript 'm' and 'f' denote matrix and fibre, respectively. The displacement at the interface, however, sustains a discontinuity δ_{if}

$$\delta_{\mathrm{if}} = u_z^{\mathrm{m}}(r=a) - u_z^{\mathrm{f}}(r=a) \tag{3}$$

The solution for the steady state is desired and therefore it is assumed that the solutions to the displacement fields can be written

$$u_z^{I}(r,\theta) = w_I(r) e^{i\omega t}\sin\theta \tag{4}$$

where I = m, f and $w_I(r)$ is an unknown function of r. Similarly, the solution to the displacement discontinuity at the interface can be assumed to be

$$\delta_{\text{if}}(\theta) = \delta_{\text{amp}} e^{i\omega t} \sin\theta \tag{5}$$

where δ_{amp} is the maximal value of interfacial sliding. This remains to be determined together with $w_I(r)$ in Equation (4) using the boundary conditions, Equations (2)-(3) and $\tau_{rz} = \tau_0 e^{i\omega t}\sin\theta$ at $r = b$, and the equilibrium and constitutive relations given in He and Liu [7]. Once the displacement field is known, the shear stress at the interface can then be computed from

$$\tau^* = -\frac{G_{\text{m}}^*}{1+\alpha^*+(1-\alpha^*)V_{\text{f}}}\left[(1-V_{\text{f}})\frac{\delta_{\text{amp}}}{a} - \frac{2\tau_0}{G_{\text{m}}^*}\right] e^{i\omega t}\sin\theta \tag{6}$$

where $\alpha^* = G_{\text{m}}^* / G_{\text{f}}$, G_{f} is the elastic shear modulus of the fibres and G_{m}^* is the complex shear modulus of the matrix. Thus, $G_m^* = G_m'(1 + i\tan\delta_m)$, where G_m' is the storage modulus and $\tan\delta_m$ the loss factor of the matrix. The shear strain in the STF layer is assumed to be uniform, i.e. $\gamma = \delta_{\text{amp}}/h$. The assumption that the shear strain is uniform around the fibre (i.e. no θ dependence and STF is in the same state around the fibre) affects the viscosity, and in a more accurate model, this has to be taken into consideration. The shear strain can be obtained by combining Equation (1) with Equations (5)-(6) as

$$\gamma = \frac{2\tau_0 a}{h(1-V_{\text{f}})G_{\text{m}}^*}\frac{1-i\omega x}{1+\omega^2 x^2} \tag{7}$$

where x is a parameter given by

$$x = \frac{1+\alpha^*+(1-\alpha^*)V_{\text{f}}a}{(1-V_{\text{f}})G_m^* h}\eta \tag{8}$$

It is known that the STF viscosity depends both on γ and ω, and that η can vary over several orders of magnitude as the strain-frequency combination is changed [5]. Nevertheless, for a given γ, the linear relation in Equation (1) can be applied and η may be considered a function of ω. STFs show a unique strain independent power-law decrease in the viscosity as function of frequency, both below and above the shear-thickening transition which occurs at a critical shear strain γ_{c} [5, 6]. It is therefore assumed that the STF viscosity η as function of the frequency, i.e. $f = \omega / 2\pi$, can be described by

$$\eta(f) = \begin{cases} \eta_{\text{l}} f^{k_{\text{l}}} \\ \eta_{\text{h}} f^{k_{\text{h}}} \end{cases} \tag{9}$$

below and above the transition state, respectively. At the onset of thickening when the shear strain has reached the critical value corresponding to a critical frequency, f_{c}, the viscosity changes abruptly and is assumed to follow a relation

$$\eta(f) = \eta_{\text{l}} f_{\text{c}}^{k_{\text{l}}-1} f^{k_{\text{tr}}},\ f_{\text{c}} \le f \le \left(\eta_{\text{l}}\eta_{\text{h}}^{-1} f_{\text{c}}^{k_{\text{l}}-1}\right)^{-(k_{\text{tr}}-k_{\text{h}})^{-1}} \tag{10}$$

i.e. until the viscosity reaches the post-transition value given in Equation (9). The coefficients, η_{l}, η_{h}, k_{l}, k_{h} and k_{tr} to describe the functions in Equation (9)-(10) and $\gamma_{\text{c}}(f)$ can be obtained from oscillatory rheology measurements at different shear strain amplitudes as in Fischer et al. [5].

Finally to obtain the dynamic effective shear modulus of the composite, the periodic average stress $\langle \tau_{32} \rangle$ and average strain $\langle \gamma_{32} \rangle$ are computed using the relations for the stress and displacement field in the composite cylinder [7]. The complex effective shear modulus of the composite is then given by $G_{\text{c}}^* = \langle \tau_{32} \rangle / \langle \gamma_{32} \rangle = G_{\text{c}}'\left(1 + i\tan\delta_{\text{c}}\right)$, where

G_c' and $\tan\delta_c$, are is the storage modulus and the damping of the composite, respectively. Analytical expressions are obtained, but for the case of a viscoelastic matrix, the expressions become large and difficult to comprehend. However, when the matrix and fibre both are elastic, simple analytical expressions are obtained as shown here for the damping of the composite

$$\tan\delta_c = \frac{4V_f\omega x}{4V_f + \left(1+\alpha-2V_f+V_f^2(1-\alpha)\right)(1+\omega^2x^2)} \qquad (11)$$

where $\alpha = G_m / G_f$, and G_m is the elastic shear modulus of the matrix. Equation (11) reveals that the effective damping of a composite with a viscous interface depends on several factors such as V_f, ω, α, a/h, η, and G_m. These parameters together with the amplitude of the applied external force F_a are needed as input to the modelling.

3. EXPERIMENTS

Dynamic mechanical analysis (DMA) was carried out to experimentally validate the model's predictive capability. Composites containing STF at the interface between its two constituent phases were designed particularly for this purpose.

The STF was composed of spherical monodisperse particles (KE-P50, Nippon Shokubai Co.) with an average particle size of 500 nm. The carrier fluid was polyethylene glycol (PEG) ($H(OCH_2CH_2)_nOH$) with an average molar mass of 200 g/mol (Sigma-Aldrich). After adding the carrier fluid to the dry powder, the suspension was roll-mixed over night, before putting it in a vacuum chamber for several hours to eliminate air bubbles. The solids concentration was set to 67.75 %w/w. The rheological properties of the STF, i.e. $\eta(f)$ in Equation (9)-(10), were determined with rheological measurements performed on a strain-controlled Advanced Rheometric Expansion System (ARES) rheometer (Rheometric Scientific). Dynamic frequency sweeps were carried out using 25 mm diameter parallel plates with a gap of 400 μm.

Composite samples (10×7×3 mm), shown in Figure 2a, were made of a silicone matrix (Elastosil M4470, Wacker Inc.) and glass fibre-epoxy rods (Swiss Composites). The stiff rods were use as reinforcing phase since there exists no common way to (*i*) coat conventional reinforcing fibres with STFs, and (*ii*) control interfaces of the order of magnitude of the fibre radius. Silicone samples with holes were moulded and then filled with STF. After the glass fibre-epoxy rods were gently introduced into the STF filled holes, from one side of the sample while the other side was sealed in order to guarantee fluid at the interface between the silicone and the rods. The compliant matrix was chosen to be able to induce significant shear deformations at the interface and obtain thickening under the used testing conditions. For an applied shear stress, the shear strain in the STF layer, given in Equation (7), depends largely on the ratio of the STF layer thickness by the fibre radius, a/h. Considering this and that the model used here is valid only for an interface thickness negligible compared to the fibre radius, i.e. Equation (1), rods with a radius of $a = 1$ mm were chosen and the STF layer thickness was approximately $h = 50$ μm. The obtained volume fraction of the fibres was $V_f = 0.25$.

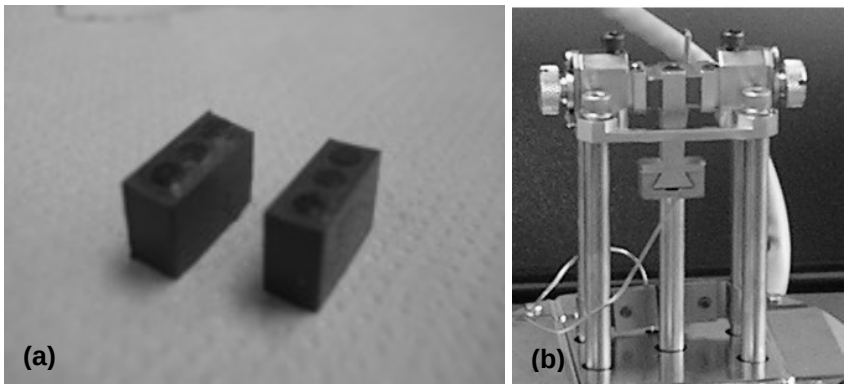

Figure 2: (a) Composite samples made of a silicone matrix and glass fibre-epoxy rods coated with STF. (b) Shear clamp used in dynamic mechanical testing.

The dynamic behaviour of both the matrix material and the composite samples was experimentally determined. Dynamic mechanical data were obtained with a DMA Q800 (TA Instruments) using the shear sandwich mode at various frequencies, f, and force amplitudes, F_a. The shear sandwich clamp of the DMA is shown in Figure 2b. The shear stress amplitude τ_0 (Figure 1a) relates to the external applied force amplitude, F_a, as $\tau_0 = F_a/2A$, where A is the area of the longitudinal section of the sample. Both frequency sweeps at constant amplitude and stress sweeps at constant frequency were made for a range of frequency $f = 0.1$-100 Hz and for force amplitudes $F_a = 0.1$, 0.3, 0.6, 0.9, 1, 1.1, 1.2, 1.5 N.

4. EXPERIMENTAL RESULTS

4.1 Rheology of shear thickening fluids

Figure 3a shows the dynamic viscosity of the STF, $\eta(f)$, at different strain amplitudes. The results are consistent with other experiments on the same material system [6]. The pre- and post-transition viscosity, shown in Figure 3b and Figure 3c, respectively, is as expected independent of the applied strain amplitude in frequency sweeps. A unique power-law decrease in the viscosity with frequency is seen both below and above the shear-thickening transition (Figure 3a-c). Figure 3b-c show the corresponding fit from which the coefficients in Equation (9) were determined. It should be mentioned that the STFs showed a brittle post-transition behaviour, often leading to fracture of the specimens. Because the viscosities in some cases were out of the range of a conventional rheometer after thickening, the post-transition behaviour at high shear strain amplitudes (Figure 3a and Figure 3c) could not be properly investigated.

The transition behaviour seen in Figure 3d can be considered to follow a similar trend line irrespective of the shear strain at which the thickening occurs, i.e. in log-log scale the curves are almost parallel with a positive slope. The power law exponent k_{tr} in Equation (10), i.e. the slope of the transition lines in Figure 3a, was determined by fitting to each transition line. An average value of $k_{tr} = 2.2$ was obtained. The coefficients that describe the pre- and post-transition behaviour are shown in Figure 3b-c. In Figure 3d the critical shear strain for thickening as function of the frequency is shown. The values, taken from Fischer [6], are based on numerous measurements on a STF having the same characteristics as the one used in this work. A linear relation in log-log scale is obtained and the corresponding fit shown in Figure 3d was used to determine the critical transition frequency f_c for any given strain amplitude.

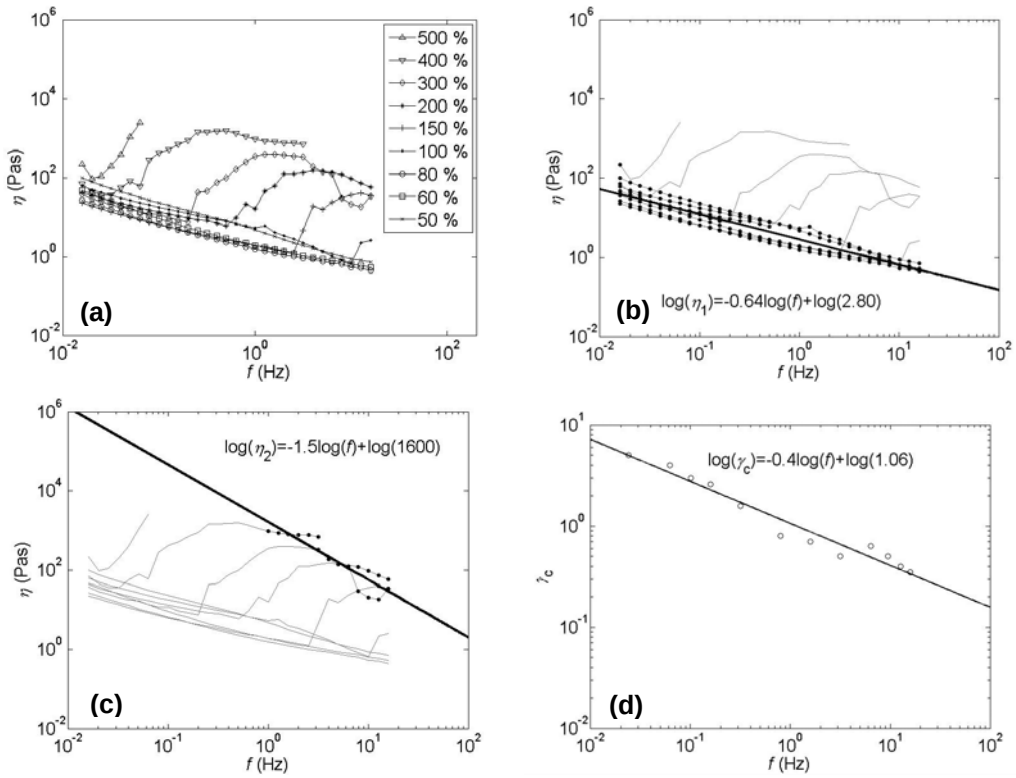

Figure 3: (a) The dynamic viscosity of a STF of 67.75 %w/w silica particles in PEG. (b) Pre-transition and (c) post-transition behaviour. (d) The critical shear strain for thickening.

4.2 Dynamic mechanical analysis

The dynamic properties of the matrix material were determined first. The silicone matrix was tested at $F_a = 0.5$, 1.0 N. It was seen that the shear storage modulus G'_m and the shear damping ratio $\tan\delta_c$ did not vary significantly with f and F_a. A mean value of $G_m^* = 0.37(1+i0.04)$ MPa was obtained from these experiments. It should be mentioned that results of the DMA testing were strongly dependent on clamping conditions. Two extreme clamping conditions, i.e. the minimum required and a very high clamping force, were tested for the neat silicone matrix. The average storage modulus over a frequency range from 0.1 to 100 Hz, increased with as much as 40% at higher clamping force testing conditions. The difference in the damping ratio was lower, however the average value of over the frequency range decreased almost by 20% when a high clamping force was applied.

Figure 4a-b shows DMA results of the composite with STF at the matrix-rod interface. The straight horizontal lines correspond to the values of the neat silicone matrix. It can be seen in Figure 4a-b that the composite dynamic properties exhibited a strong dependence on both F_a and f, in particular in the low frequency range from 0 to 20 Hz. The peaks observed at low f for the high F_a, in Figure 4b, suggested that the STF had thickened and thus significantly affected the composites overall damping, increasing $\tan\delta_c$ compared to the results obtained at low F_a. The viscosity of the STF (Figure 3a) increases with the shear strain amplitude. When F_a is increased, the shear strain in the STF layer, cf. Equation (7), also increases which translates into a viscosity increase. The remarkable increase in damping ratio indicates that the STF is in transition, or post-transition, state where it is know that a great amount of viscous dissipation takes place [4].

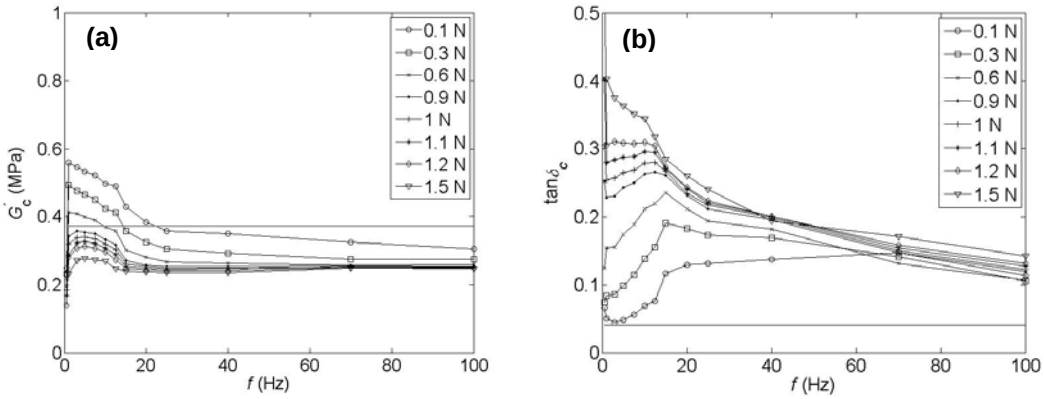

Figure 4: Experimentally determined dynamic properties of the composite containing STF in terms of the (a) storage modulus, and (b) loss tangent.

A closer look at Figure 4a-b reveals and an increase in G'_c and a decrease in $\tan\delta_c$ with f at constant F_a. At constant f, a decrease in G'_c and an increase in $\tan\delta_c$ with increasing F_a, was observed. An increase in G'_c with frequency at constant F_a could be due to thickening of the STF which improves the stress transfer between the rods and the matrix. However, the increase is unrealistically high, especially at low F_a, where the composite samples become stiffer than the neat matrix samples (Figure 4a) which would be the case if the rod-matrix bonding was close to perfect. Moreover, the trend of a decrease in G'_c with increasing F_a, is not consistent with the rheological properties of the STF i.e. viscosity increase with F_a at constant frequency due to larger shear strain amplitude at the interface. The values of G'_c, especially for low F_a, cannot be considered reliable. Possible sources of error induced by the experimental setup, i.e. clamping device, are among others (*i*) non-uniform interface thickness, due to sample deformation, and (*ii*) friction, due to direct contact between the matrix and the rods created by sample deformation which reduces the STF layer thickness to zero where maximum shear strain occurs (Figure 2b). Moreover boundary effects, due to the particular configuration of the sample (Figure 2a), could lead to complex stress states and unexpected results.

5. COMPARISON BETWEEN MODEL PREDICTIONS AND EXPERIMENTS

The model was run with values of F_a corresponding to the experimental ones over a frequency rage from 0.01 to 100 Hz. Simulations were performed with the input data given in Table 1.

Table 1. Input data used for modelling.

Microstructure			**Constituent properties**						
a	h	V_f	G_f	G^*_m	$\eta(f)$				
(mm)	(μm)	(%)	(GPa)	(MPa)	η_l	k_l	η_h	k_h	k_{tr}
1	50	25	30	$0.37(1+i0.04)$	2.8	−0.64	1600	−1.5	2.2

The predicted G'_c and $\tan\delta_c$ for silicone based STF composites is shown in Figure 5a-b. For $\tan\delta_c$ good qualitative and quantitative agreement with experimental results was obtained (cf. Figure 4b and Figure 5b). The predicted G'_c is as expected lower than the one of the matrix material due to imperfect interface. A slight increase in G'_c with f at constant F_a is seen in the low frequency range. As opposed to the experimental results,

predicted G'_c increased with F_a at constant frequency due to increase in shear strain at the interface, and hence STF viscosity increase. It was mentioned previously that experimental values of G'_c at low F_a cannot be considered reliable. Predicted G'_c values are comparable to the experimental ones only at high force amplitudes, e.g. F_a = 1.5 N.

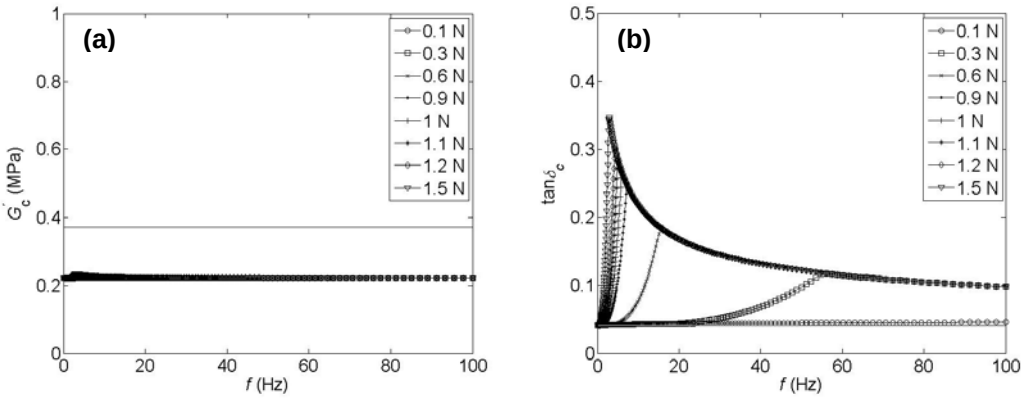

Figure 5: Predicted dynamic properties of the composite containing STF in terms of the (a) storage modulus, and (b) loss tangent.

Figure 6a shows the predicted and the experimentally determined tanδ_c for three different F_a. The peaks in the model, for the higher F_a correspond to thickening of the STF (Figure 3a). Therefore, the model confirmed that the damping peaks coincided with the thickening of the STF at the matrix-rod interface. Since the thickening onset of STFs occurs at lower f as shear strain is increased (Figure 3d), the damping peak was moved to lower frequencies with increasing F_a (Figure 5b and Figure 6a). Furthermore, the fact that the post-transition viscosity significantly decreases with increasing f (Figure 3c) clearly affected the damping behaviour of the silicone matrix composite, which followed a similar behaviour.

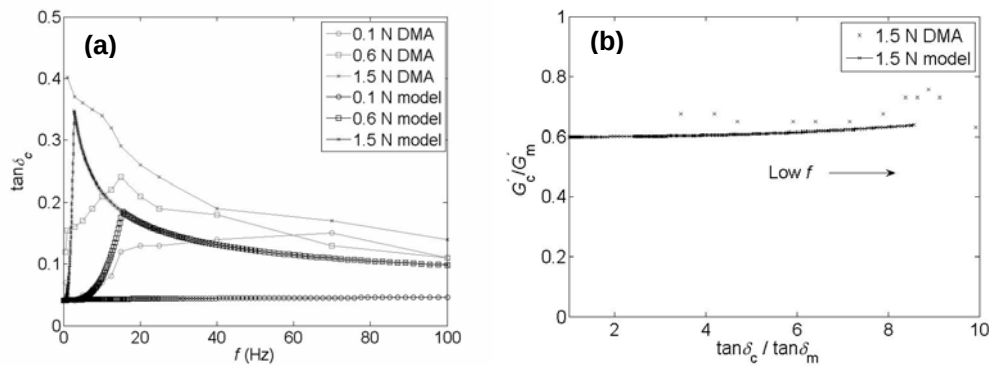

Figure 6: (a) Loss factor vs. frequency as determined by DMA experiments compared with model predictions. (b) Stiffness-loss map for the composite containing STF for f = 0.1-100 Hz and F_a = 1.5 N.

It can be concluded that damping peaks appear and their location depends on the onset of thickening and post-thickening behaviour. With the behaviour of the STF used in this particular case, the maximum increase in damping will occur at low frequencies for high force amplitudes. Once the STF is thickened at low frequencies, the viscosity changes with higher frequencies leading to a decrease in damping as can be seen in Figure 6a. Hence the increase in damping due to thickening of STF at higher frequencies will not be so dramatic, and it will follow the corresponding viscosity change in the transition state of the STF from a lower bound (e.g. at low force

amplitude of 0.1 N in Figure 6a) to an upper bound given by the behaviour in the thickened state (e.g. curves for high force amplitude in Figure 6a).
The simulations show that the effect of a viscous interface on the damping of composites is considerable. Figure 6b shows a normalized stiffness-loss map over the tested frequency range and $F_a = 1.5$ N. The great improve in damping is striking, however the stiffness is decreased. Nevertheless, the stiffness-damping behaviour can be tailored by properly adjusting the interface viscosity, i.e. $\eta(f)$, the ratio a/h, the fibre volume fraction and the matrix stiffness, independently or jointly, for a certain vibration frequency.

6. CONCLUSIONS

A micromechanical model developed for composite materials with a STF at the fibre-matrix interface showed good agreement with experimental DMA results. The damping of the composites was improved significantly. The dynamic properties exhibited a strong dependence on both frequency and applied external load amplitude. Damping peaks appeared which coincided with the thickening of the STF at the matrix-rod interface. The location of the peaks depends on the onset of thickening and post-thickening rheological behaviour of the STF. Composite materials with STF integrated at the fibre matrix interface offer the possibility of tailoring the stiffness-damping behaviour for a certain vibration frequency by properly adjusting the STF viscosity, the constituent mechanical properties and the microstructure, independently or jointly.

ACKNOWLEDGEMENTS

The authors gratefully acknowledge the Sports and Rehabilitation Engineering (SRE) program of the EPFL for financial support, Jérôme Durivault for help to validate the model and Sebastien Lavanchy for technical support.

REFERENCES

1- Chandra, R., Singh, S. P., and Gupta, K., “Damping studies in fiber-reinforced composites - a review”, *Composite Structures*, 1999;46:41-51.
2- Finegan, I. C., and Gibson, R. F., “Recent research on enhancement of damping in polymer composites”, *Composite Structures*, 1999;44:89-98.
3- Fischer, C., Braun, S. A., Bourban, P.-E., Michaud, V., Plummer, C. J. G., and Månson, J.-A. E., “Dynamic properties of sandwich structures with integrated shear-thickening fluids”, *Smart Materials and Structures* 2006;15:1467-1475.
4- Lee, Y. S., and Wagner, N. J., “Dynamic properties of shear thickening colloidal suspensions”, *Rheologica Acta*, 2003;42:199-208.
5- Fischer, C., Plummer, C. J. G., Michaud, V., Bourban, P.-E., and Månson, J.-A. E., “Pre- and posttransition behaviour of shear thickening fluids in oscillating shear”, *Rheologica Acta*, 2007;46:1099-1108.
6- Fischer, C., 2007. Adaptive composite structures for tailored human-materials interaction., Thèse EPFL, no 3890. Dir.: Jan-Anders E. Månson, Pierre-Etienne Bourban.
7- He, L. H., and Liu, Y. L., “Damping behavior of fibrous composites with viscous interface under longitudinal shear loads”, *Composites Science and Technology*, 2005;65:855-860.
8- Hashin, Z., “Analysis of composite materials - A survey”, *Journal of Applied Mechanics*, 1983;50:481-505.
9- Hashin, Z., “Analysis of properties of fiber composites with anisotropic constituents”, *Journal of Applied Mechanics*, 1979;46:543-550.